Additional file 1

Decoding the dynamics of cellular metabolism and the action of 3-bromopyruvate and 2-deoxyglucose using pulsed stable isotope-resolved metabolomics

Pietzke and Zasada et al., Cancer and Metabolism 2014

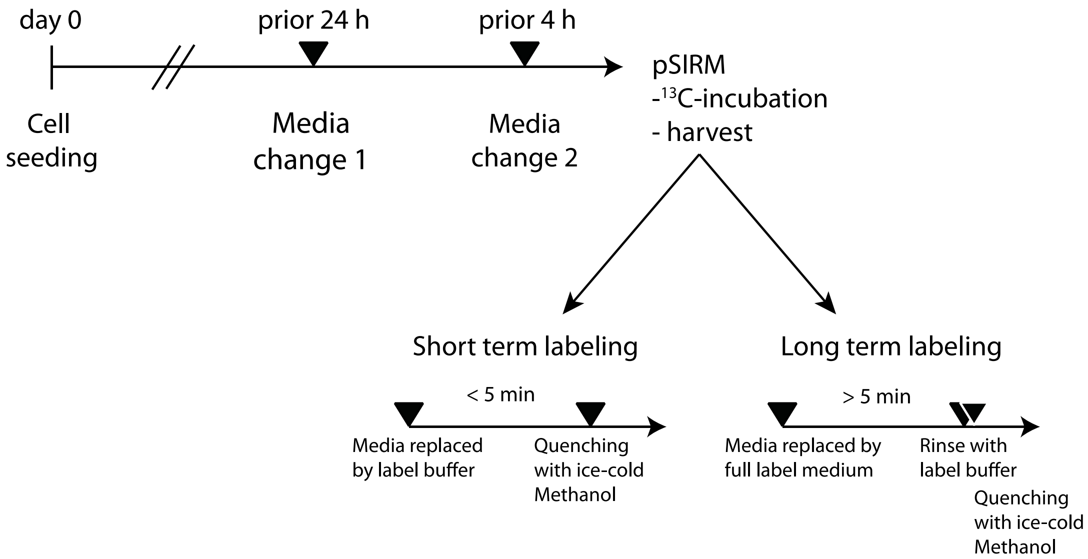

Figure S 1 - Experimental setup of harvesting procedure for a pSIRM cell culture experiment.

Cells are seeded with pre-determined cell number to avoid growth inhibitory effects until harvest on day 3 of the experiment. Media is replaced to supply cells with nutrients 24 and 4 hours prior the harvest. The harvest protocol summarizes the labeling procedure of adherent cell cultures (see Methods section).

Additional file 1

Decoding the dynamics of cellular metabolism and the action of 3-bromopyruvate and 2-deoxyglucose using pulsed stable isotope-resolved metabolomics

Pietzke and Zasada et al., Cancer and Metabolism 2014

Table S 1 – Composition of the full label medium and label buffer for pSIRM experiments used for the labeling of T98G cells and other cell lines as mentioned in the manuscript.

	Full label medium	Label buffer
Base	Dulbeccos modified eagle medium (DMEM) - without Glucose - without Glutamine - without Pyruvate	HEPES (5 mM) NaCl (140 mM) pH 7.4
Carbon sources	+ ^{13}C-Glucose (2.5 g/L) + ^{12}C-Glutamine (4 mM)	+ ^{13}C-Glucose (2.5 g/L) + ^{12}C-Glutamine (4 mM)
Supplemented with	+ small molecules (inhibitor, antibiotics etc.)	

Additional file 1
Decoding the dynamics of cellular metabolism and the action of 3-bromopyruvate and 2-deoxyglucose using pulsed stable isotope-resolved metabolomics
Pietzke and Zasada et al., Cancer and Metabolism 2014

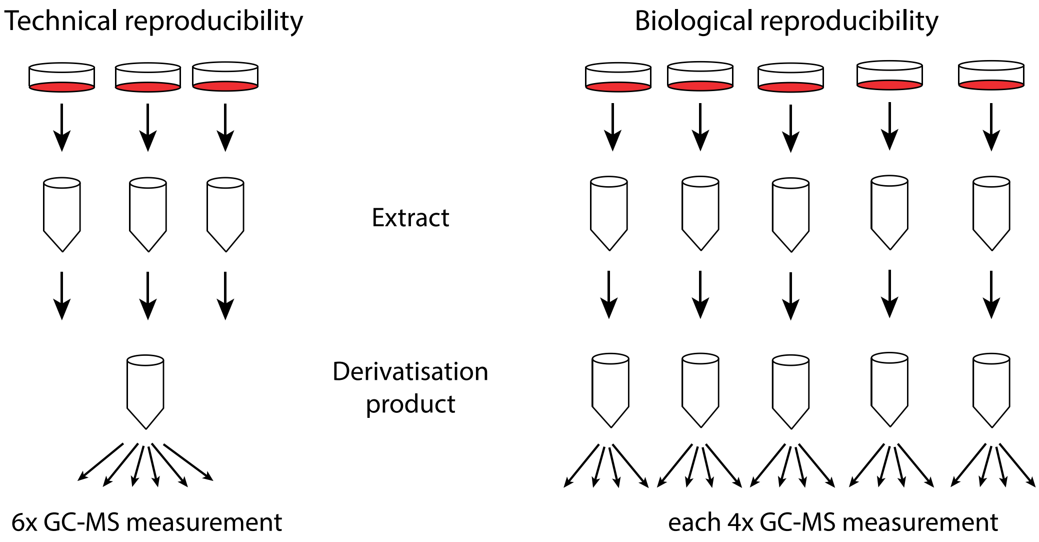

Figure S 2 – Experimental scheme of the reproducibility experiment to determine technical and biological variances of GC-MS derived data.
T98G cells were cultured for three days, and labeled with ^{13}C-glucose for 3 minutes. Cell extracts were prepared separately for each cell culture plate. Technical variance was determined by the repeated measurement of pooled cell samples. Biological reproducibility was determined by repeated measurement of five independently treated cell samples.

Additional file 1
Decoding the dynamics of cellular metabolism and the action of 3-bromopyruvate and 2-deoxyglucose using pulsed stable isotope-resolved metabolomics
Pietzke and Zasada et al., Cancer and Metabolism 2014

Table S 2 – Biological and technical variation of the measurement of metabolite pool sizes in T98G cells.
The coefficient of variation (CoV) of the peak area for each metabolite was calculated from six consecutive measured technical replicates. The calculation of CoVs for the biological reproducibility based on five biological replicates, each measured in four technical repetitions.

	Coefficient of variation	
Compound	**Technical replicates**	**Biological replicates**
Adenine	13.7	14.7
Alanine, beta-	8.9	12.4
Alanine	6.8	10.0
Asparagine	9.0	5.3
Aspartic acid	3.6	10.3
Butanoic acid, 2-amino-	9.3	5.5
Butanoic acid, 3-hydroxy-	7.6	15.9
Butanoic acid, 4-amino-	16.1	19.6
Citric acid	8.9	10.6
Cytosine	15.1	12.1
Fructose-1,6-bisphosphate	15.3	15.6
Fructose	11.5	13.9
Fructose-6-phosphate	6.4	10.3
Fumaric acid	9.0	10.4
Glucose	8.6	7.0
Glucose-6-phosphate	10.8	11.6
Glutamine	5.9	11.9
Glutaric acid, 2-hydroxy-	8.7	13.4
Glutaric acid, 2-oxo-	12.2	14.3
Glyceric acid	6.3	7.1
Glyceric acid-3-phosphate	11.3	14.7
Glycerol	15.3	16.5
Glycerol-3-phosphate	10.2	13.1
Glycine	12.7	6.6
Inositol, myo-	11.3	11.6
Isoleucine	8.1	12.0
Lactic acid	3.9	11.0
Leucine	7.6	8.6
Lysine	12.0	11.5
Malic acid	9.2	13.3
Methionine	16.8	20.7
Pantothenic acid	11.2	11.2
Phosphoenolpyruvic acid	11.8	13.2
Proline	7.6	5.2
Putrescine	14.5	8.1
Pyroglutamic acid	10.1	13.8
Pyruvic acid	5.3	7.5
Ribitol	11.5	9.3
Ribose-5-phosphate	11.3	11.2
Serine	10.0	10.2
Succinic acid	15.0	21.3
Sucrose	23.2	29.5
Threonine	10.4	11.1
Tyrosine	10.7	8.2
Uracil	10.0	20.5
Uridine 5'-monophosphate	6.8	14.3
Uridine	21.5	13.5
Valine	5.6	11.6

Table S 3 – Quant mixture composition and concentration range for each metabolite

	Concentration range in Quant mix (pmol)	
Compound	**Minimum**	**Maximum**
Adenine	37	7400
Adenosine	94	18709
Alanine	673	134695
Alanine, beta	56	11225
Arginine	57	11481
Asparagine	114	22707
Aspartic acid	75	15025
Butyric acid, 3-hydroxy	144	28818
Butyric acid, 4-amino	48	9697
Citric acid	260	52051
Creatinine	221	44201
Cysteine	41	8254
Cytosine	45	9001
Dihydroxyacetone phosphate	441	88183
Erythritol, meso	409	81887
Fructose	416	83259
Fructose-1,6-bisphosphate	271	54288
Fructose-6-phosphate	66	13154
Fumaric acid	172	34462
Gluconic acid-6-phosphate	73	14616
Glucosamine	23	4638
Glucose	1943	388544
Glucose 1-phosphate	59	11894
Glucose-6-phosphate	164	32884
Glutamic acid	680	135934
Glutamine	684	136855
Glutaric acid	151	30278
Glutaric acid, 2-hydroxy	286	57268
Glutaric acid, 2-oxo	171	34223
Glyceraldehyde-3-phosphate	323	64668
Glyceric acid	80	15987
Glyceric acid-3-phosphate	217	43478
Glycerol	326	65154
Glycerol-3-phosphate	135	26996
Glycine	333	66605
GMP	101	20113
Hypotaurine	92	18323
Inosine	56	11184
Inositol, myo	278	55506
Isoleucine	191	38116
Lactic Acid	2231	446190
Leucine	457	91484
Lysine	103	20531
Malic acid	224	44746
Methionine	34	6702
Pantothenic acid	84	16788
Phenylalanine	242	48429
Phosphoenolpyruvic acid	75	15036
Proline	304	60801
Putrescine	31	6208
Pyroglutamic acid	465	92937

Pyruvate	1454	290803
Ribose	100	19983
Ribose, 2-deoxy	37	7455
Ribose 5-phosphate	456	91208
Serine	571	114188
Succinic acid	212	42341
Threonine	839	167898
Tryptophan	49	9793
Tyrosine	55	11038
Uracil	134	26764
Uridine 5′-monophosphate	407	81489
Valine	213	42680

Additional file 1
Decoding the dynamics of cellular metabolism and the action of 3-bromopyruvate and 2-deoxyglucose using pulsed stable isotope-resolved metabolomics
Pietzke and Zasada et al., Cancer and Metabolism 2014

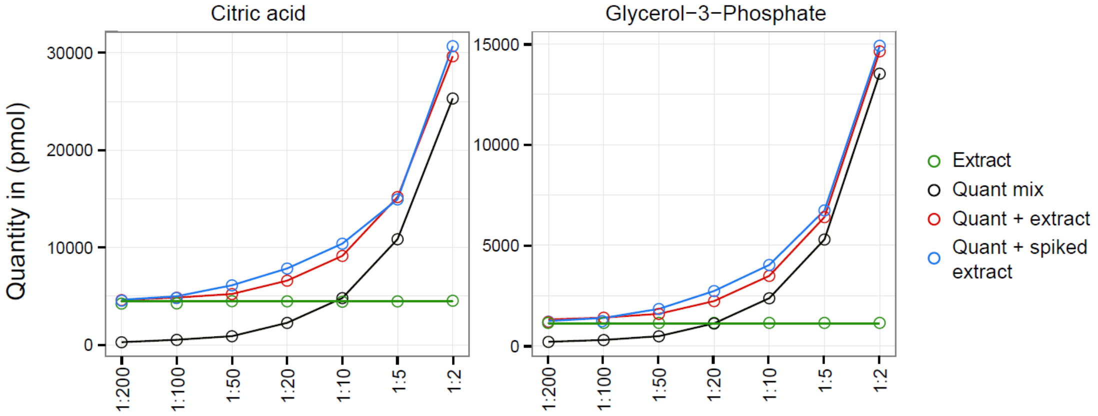

Figure S 3 - Illustration of quant-addition experiment**.**
The measurement of the quant mixture delivers calibration curves, which were used to quantify the biological sample – here shown for citric acid and glycerol-3-phosphate. The quantification results are shown for the individual measurements of quantification mixtures (black), cell samples (green), the sum of quantities of cell extracts and quantification mixtures (red), and the measurements of samples spiked into quantification mixtures (blue).

Additional file 1

Decoding the dynamics of cellular metabolism and the action of 3-bromopyruvate and 2-deoxyglucose using pulsed stable isotope-resolved metabolomics

Pietzke and Zasada et al., Cancer and Metabolism 2014

Table S 4 – Data quant addition experiment. T98G cell extracts, equivalent to 7.14 x 10^5 cells, were quantified by external quantification. Same amounts of extracts were spiked into each dilution of the quantification mixture.

Compound	Concentration in extract in pmol (Avg ± SD)			Conc. quant (measured) + conc. extract (pmol)							Conc. (Quant + spiked in extract) (pmol)						
				1:200	1:100	1:50	1:20	1:10	1:5	1:2	1:200	1:100	1:50	1:20	1:10	1:5	1:2
Adenine	614	±	182	614	614	807	950	1371	2184	4220	697	576	791	1128	1466	2032	4422
Alanine, beta-	2300	±	624	2300	2434	2560	2883	3456	4497	8130	2078	1987	2275	2722	3115	4105	6419
Alanine	9840	±	3183	10689	11537	12291	16541	24554	36271	83215	11637	8756	11316	15642	22001	34702	83667
Butanoic acid, 3-hydroxy-	213	±	88	370	529	780	1717	3263	5977	16149	458	507	1000	2238	4209	7850	19883
Citric acid	4333	±	330	4609	4855	5225	6596	9141	15188	29647	4635	4992	6119	7847	10398	14948	30685
Cytosine	1467	±	326	1467	1753	1857	1994	2347	3224	5995	1492	1585	1975	2649	3233	4266	7492
Erythritol	1403	±	147	1869	2266	2987	5228	9093	17585	43782	1813	2390	3651	6710	11466	21274	49021
Fructose BP	9224	±	473	9678	10060	10707	12880	17166	26803	49782	9809	10729	12542	15474	19566	27418	50961
Fructose MP	8791	±	793	9225	9615	10287	12481	16838	26351	50400	9334	10040	11675	14497	18623	26486	51298
Fructose-6-phosphate	326	±	37	457	533	613	912	1501	2980	7169	311	363	436	723	1118	2030	4996
Fumaric acid	1234	±	93	1431	1617	1929	2848	4585	8242	18609	1462	1744	2357	3621	5852	9728	20213
Glucose-1/6-phosphate	1137	±	207	1494	1613	1915	2881	4954	10100	24578	1332	1489	1837	3155	5141	8372	19299
Glutaric acid, 2-hydroxy-	396	±	25	680	960	1531	3345	6495	12605	29013	783	1277	2410	5245	9134	15837	33714
Glutaric acid, 2-oxo-	6150	±	380	6150	6529	6787	7852	9624	13348	22607	6284	6766	7550	8952	10693	13739	22961
Glutaric acid	136	±	51	265	443	733	1618	3248	6360	15488	317	561	1002	2319	4442	8281	18164
Glyceric acid	223	±	24	299	377	521	1001	1792	3463	8443	309	439	696	1398	2476	4456	9674
Glyceric acid-3-phosphate	875	±	139	875	1436	1628	2795	4864	9482	22350	1090	1196	1697	2860	4455	7944	19644
Glycerol	4305	±	369	4568	4981	5732	7979	11706	17908	37709	4785	5242	6415	9767	13930	22057	45069
Glycerol-3-phosphate	1111	±	142	1315	1406	1594	2228	3482	6402	14642	1236	1389	1839	2729	4025	6736	14917
Glycine	12759	±	3200	13085	13507	14327	16497	20261	26574	46330	12253	10957	12341	15094	17442	22535	36278
Hypotaurine	2551	±	273	2665	2770	2913	3438	4502	6506	11552	2617	2751	3241	4034	5103	6938	12927
Inositol, myo-	7313	±	885	7655	7878	8301	9637	12310	18742	35335	7811	8279	9033	11657	14604	21199	39071
Lactic acid	189454	±	18268	192498	194432	197362	208360	229315	280861	432389	194868	195966	218580	246012	269882	310055	424055
Leucine	16789	±	3287	16789	17776	18899	22799	28801	35738	63458	18069	16244	20882	25246	30916	37820	63263
Malic acid	5428	±	321	5676	5884	6262	7462	9561	14172	27697	5682	6436	7568	9418	12320	17703	32113
Pantothenic acid	1396	±	244	1488	1569	1715	2175	2990	4917	9710	1597	1740	2090	3099	4038	6077	11764
Phenylalanine	10229	±	2156	10632	10823	11110	12534	15479	20126	35598	10559	10023	11674	13275	15093	17457	34055
Proline	7661	±	1824	7661	7962	8766	12088	17110	20495	39253	8525	7189	10088	13832	18334	24202	43926
Putrescine	151	±	12	198	238	311	499	823	1412	3415	186	221	325	552	872	1552	3353
Pyroglutamic acid	58365	±	4119	58818	59351	60187	62939	67892	77985	105173	56276	61889	68508	76717	83975	97376	125674
Pyruvic acid	31775	±	5243	32523	35292	38762	48600	66948	95473	178251	35120	35723	44233	64988	98394	141628	259046
Ribose	91	±	27	183	289	502	1086	2114	4566	9154	230	347	656	1313	2422	4185	8674
Serine	23025	±	3328	23674	24376	25174	28578	35000	45122	82883	24334	24116	28823	35298	42207	53976	93783
Succinic acid	1801	±	134	2011	2260	2679	4098	6439	10545	23352	2040	2373	3233	5268	8186	13249	26145
Threonine	36780	±	5628	37576	38779	40274	45846	56066	71285	125978	38110	37739	45000	55794	67967	91359	158356
Uracil	4135	±	2397	4135	4403	4722	5428	6721	9606	17499	2044	1258	900	1887	4457	6908	14402
Valine	11337	±	2111	11559	11847	12214	13616	15970	19668	35039	11936	11267	14342	16885	19559	23046	33794

Table S 5 - Recovery of metabolites

The recovery is defined as ratio of the quantity of spike-in and summed up quantities of individual measured quantification mixtures and extracts. The recovery was calculated at equal concentrations of quantification mixture and extracts.

Compound	Recovery (%)
Adenine	112.9
Alanine, beta-	91.3
Alanine	92.1
Butanoic acid, 3-hydroxy-	109.8
Cinnamic acid, trans-	104.7
Citric acid	116.4
Cytosine	132.3
Erythritol	122.2
Fructose BP	108.1
Fructose MP	110.6
Fructose-6-phosphate	75.3
Fumaric acid	102.2
Glucose-1/6-phosphate	102.7
Glutaric acid, 2-hydroxy-	124.1
Glutaric acid, 2-oxo-	107.0
Glutaric acid	119.6
Glyceric acid	125.0
Glyceric acid-3-phosphate	104.2
Glycerol	111.9
Glycerol-3-phosphate	122.5
Glycine	84.8
Hypotaurine	113.4
Inositol, myo-	115.9
Lactic acid	104.2
Leucine	106.6
Malic acid	126.9
Pantothenic acid	135.1
Phenylalanine	86.7
Proline	110.8
Putrescine	104.5
Pyroglutamic acid	119.5
Pyruvic acid	148.3
Ribose	125.6
Serine	119.6
Succinic acid	124.6
Threonine	128.2
Uracil	69.1
Valine	106.8

Additional file 1
Decoding the dynamics of cellular metabolism and the action of 3-bromopyruvate and 2-deoxyglucose using pulsed stable isotope-resolved metabolomics
Pietzke and Zasada et al., Cancer and Metabolism 2014

Table S 6 – Intracellular metabolite concentrations of T98G cells.
Data is derived from the reproducibility experiment (see Methods section). T98G cells were incubated with $^{13}C_6$-glucose for three minutes.

	Quantity (pmol / 10^6 cells)			**^{13}C-Quantity (pmol / 10^6 cells)**		
Compound	**Average**	**±**	**STDEV**	**Average**	**±**	**STDEV**
Adenine	77	±	15	*n.d*	±	*n.d*
Alanine	841	±	89	10.3	±	3.7
Alanine, beta-	623	±	122	*n.d*	±	*n.d*
Asparagine	202	±	15	*n.d*	±	*n.d*
Aspartic acid	251	±	22	0.4	±	0.5
Butanoic acid, 2-amino	3,965	±	702	*n.d*	±	*n.d*
Butanoic acid, 3-hydroxy	51	±	7	*n.d*	±	*n.d*
Citric acid	327	±	17	3.7	±	2
Fructose	1,068	±	32	29.0	±	2.6
Fructose-1,6,diphosphate	773	±	45	*n.d*	±	*n.d*
Fructose-6-phosphate	48	±	5	10.8	±	0.6
Fumaric acid	135	±	6	0.4	±	0.2
Glucose-6-phosphate	532	±	27	100.6	±	6.3
Glutaric acid, 2-hydroxy	98	±	5	0.5	±	0.3
Glutaric acid, 2-oxo	235	±	6	2.3	±	1.5
Glyceric acid	30	±	2	*n.d*	±	*n.d*
Glyceric-acid-3-phosphate	133	±	7	*n.d*	±	*n.d*
Glycerol-3-phosphate	90	±	5	1.6	±	0.7
Glycine	2,332	±	135	4.0	±	2.4
Inositol, myo	1,203	±	20	*n.d*	±	*n.d*
Isoleucine	1,960	±	170	*n.d*	±	*n.d*
Lactic acid	9,873	±	1,269	454.5	±	69.9
Leucine	2,409	±	134	*n.d*	±	*n.d*
Lysine	1,512	±	238	*n.d*	±	*n.d*
Malic acid	547	±	22	1.2	±	1.1
Methionine	1,009	±	74	*n.d*	±	*n.d*
Pantothenic acid	142	±	3	*n.d*	±	*n.d*
Proline	892	±	56	*n.d*	±	*n.d*
Putrescine	36	±	1	*n.d*	±	*n.d*
Pyruvic acid	195	±	31	9.3	±	1.5
Ribose-5-phosphate	185	±	11	*n.d*	±	*n.d*
Serine	2,546	±	154	*n.d*	±	*n.d*
Succinic acid	30	±	8	0.1	±	0.1
Threonine	4,971	±	339	*n.d*	±	*n.d*
Tyrosine	1,101	±	173	*n.d*	±	*n.d*
Uracil	111	±	21	*n.d*	±	*n.d*
Uridine-5-monophosphate	8,410	±	615	*n.d*	±	*n.d*
Valine	333	±	17	*n.d*	±	*n.d*

Additional file 1

Decoding the dynamics of cellular metabolism and the action of 3-bromopyruvate and 2-deoxyglucose using pulsed stable isotope-resolved metabolomics

Pietzke and Zasada et al., Cancer and Metabolism 2014

Table S 7 – Metabolite specific mass fragments for the calculation of ^{13}C-isotope incorporation. Mass fragments are chosen concerning their uniqueness for the derivate of the metabolite and were evaluated in separately performed $^{13}C_6$-glucose and $^{13}C_5$-glutamine labeling experiments.

			Mass fragment (m/z)		
Compound	**Derivate**	**Abbr.**	**Unlabeled**	**Labeling with u-^{13}C-glucose**	**Labeling with u-^{13}C-glutamine**
Alanine	3TMS	Ala	188	190	-
Aspartic acid	3TMS	Asp	232	235 (a)	-
Citric acid	4TMS	Cit	273	275	277
Dihydroxyacetone phosphate	1MeOX 3TMS	DHAP	400	403	-
Fructose	1MeOX 5TMS	Fru	217	220	-
Fructose-1,6-bisphosphate	1MeOX 7TMS	F16BP	217	220	-
Fructose-6-phosphate	1MeOX 6TMS	F6P	217	220	-
Fumaric acid	2TMS	Fum	245	247	249
Glucose	1MeOX 5TMS	Glc	319	323	-
Glucose-6-phosphate	1MeOX 6TMS	G6P	217	220	-
Gluconic acid-6-phosphate	7TMS	PG6	217	220	-
Glutamic acid	3TMS	Glu	246	-	250
Glutamine	3TMS	Gln	156	-	160
Glutaric acid	2TMS	Glut	261	-	266
Glutaric acid, 2-hydroxy	3TMS	Glut-OH	247	-	251
Glutaric acid, 2-oxo	1MeOX 2TMS	aKG	198	200	203
Glyceric acid-3-phosphate	4TMS	3PGA	357	359	-
Glycerol	3TMS	Glyc	218	221	-
Glycerol-3-phosphate	4TMS	Glyc3P	357	359	-
Glycine	3TMS	Gly	276	277	-
Lactic acid	2TMS	Lac	219	222	-
Malic acid	3TMS	Mal	233	235	236
Phosphoenolpyruvic acid	3TMS	PEP	369	372	-
Pyruvic acid	1MeOX 1TMS	Pyr	174	177	-
Ribose-5-P	1MeOX 5TMS	R5P	217	220	-
Serine	3TMS	Ser	204	206	-
Succinic acid	2TMS	Suc	247	249	251

(a) – when simultaneously applied with ^{13}C-glutamine labeling, the resulting ^{13}C-pyroglutamate might interfere with this mass range.

Additional file 1
Decoding the dynamics of cellular metabolism and the action of 3-bromopyruvate and 2-deoxyglucose using pulsed stable isotope-resolved metabolomics
Pietzke and Zasada et al., Cancer and Metabolism 2014

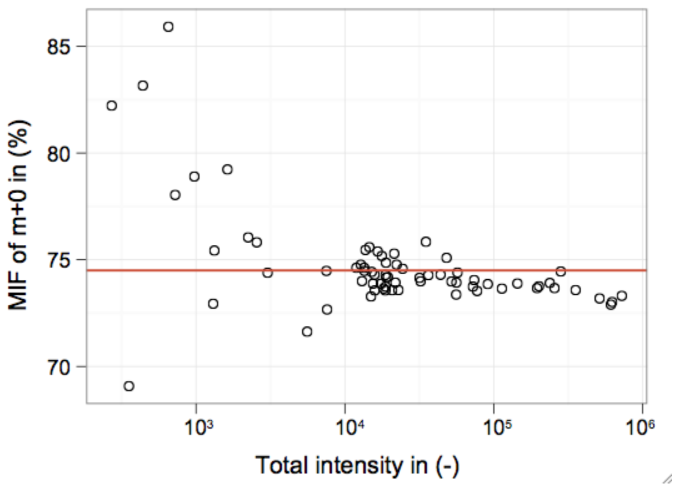

Figure S 4 - Concentration dependency of mass isotopomer fractions.
The mass isotopomer fraction (MIF) of mass fragment m+0 for citric acid (m/z = 273-279) is shown for a broad intensity range (black circles). The expected value (red line) was calculated by Mass Spec Calculator Pro Demo version 4.09 (ChemSW, Inc.). The proportion of m+0 in the mass range decreases and yields higher precision with increasing levels of citric acid.

Table S 8 – Illustration of the position dependent strategy for correction of natural ^{13}C-isotope abundance.

$^{13}C_1$-Glucose and ^{12}C-glucose were mixed in known ratios to proof the position dependent (targeted) calculation strategy. Two examples are shown for the determination of ^{13}C-incorporation as described.

		Intensities in (-)			**MIF in (%)**			**10 % $^{13}C_1$**			**50 % $^{13}C_1$**		
m/z		**^{12}C**	**10 % $^{13}C_1$**	**50 % $^{13}C_1$**	**^{12}C**	**10 % $^{13}C_1$**	**50 % $^{13}C_1$**	**S_{nat+1}**	**S_{inc+1}**	**L**	**S_{nat+1}**	**S_{inc+1}**	**L**
319	m0	156460	153425	84507	66.6	60.2	33.2						
320	**m+1**	**48250**	**63669**	**112421**	**20.6**	**25.0**	**44.2**	**18.6**	**6.4**	**9.6**	**10.2**	**33.9**	**50.5**
321	m+2	23579	28289	38071	10.0	11.1	15.0	9.1	2.0		5.0	10.0	
322	m+3	5038	7389	15467	2.1	2.9	6.1	1.9	1.0		1.1	5.0	
323	m+4	1199	1716	3268	0.5	0.7	1.3	0.5	0.2		0.3	1.0	
324	m+5	228	262	751	0.1	0.1	0.3	0.1	0.0		0.0	0.2	
	Sum	234754	254750	254485	100	100	100						

Table S 9 – Validation of correction strategies for the natural ^{13}C-carbon abundance. 1-$^{13}C_1$-Glucose (purity 99%) and unlabeled glucose were mixed in known ratios and measured in three independent replicates. Uncorrected values overestimate incorporation especially in the lower range of isotope incorporation, whereas both calculation strategies consider the natural contribution of carbon-13 correctly.

Expected isotope abundance (%)	^{13}C-abundance in glucose (%)		
	Uncorrected	**Targeted**	**Position-independent**
0	23.4 ± 0.09	0.0 ± 0.16	0.0 ± 0.12
1.98	24.7 ± 0.25	2.1 ± 0.42	2.0 ± 0.32
4.95	26.4 ± 0.21	5.0 ± 0.36	5.0 ± 0.27
9.90	29.6 ± 0.20	10.3 ± 0.33	10.1 ± 0.29
24.75	39.2 ± 0.79	25.3 ± 1.19	25.0 ± 1.26
49.50	56.8 ± 0.89	50.3 ± 1.18	49.8 ± 1.28
74.25	76.1 ± 0.78	74.2 ± 0.91	74.0 ± 0.94
89.10	89.0 ± 0.04	88.6 ± 0.04	88.4 ± 0.03
94.05	93.9 ± 0.14	93.8 ± 0.15	93.7 ± 0.15
97.02	96.8 ± 0.19	96.7 ± 0.19	96.7 ± 0.20
99.00	98.7 ± 0.04	98.7 ± 0.04	98.7 ± 0.05

Table S 10 – Biological and technical variation of ^{13}C-glucose incorporation.
T98G cells were incubated with u-^{13}C glucose for three minutes and harvested as described in the Methods section.

		Average (^{13}C-Glc incorporation in %) ± STDEV					
Compound	**Mass**	**Technical repl.**			**Biological repl.**		
3PGA	357	77.7	±	4.0	83.2	±	2.1
Ala	188	4.7	±	1.3	5.5	±	0.6
Cit	273	4.2	±	2.0	7.1	±	1.2
F16BP	217	78.8	±	1.0	79.7	±	0.7
Fru	217	10.7	±	0.7	7.7	±	0.7
F6P	217	84.0	±	4.8	83.2	±	4.0
Fum	245	0.9	±	0.7	0.6	±	0.2
G6P	217	74.6	±	0.5	74.3	±	0.4
Glut-OH	198	3.2	±	2.4	1.5	±	1.6
Glyc3P	357	6.7	±	2.7	8.9	±	1.3
Gly	276	0.2	±	0.6	*n.d.*	±	*n.d.*
Lac	219	17.9	±	0.4	18.4	±	2.7
Mal	245	0.7	±	0.7	0.2	±	1.1
Pyr	174	18.9	±	3.0	17.3	±	1.3
Suc	247	*n.d.*	±	*n.d.*	1.0	±	1.2

Additional file 1
Decoding the dynamics of cellular metabolism and the action of 3-bromopyruvate and 2-deoxyglucose using pulsed stable isotope-resolved metabolomics
Pietzke and Zasada et al., Cancer and Metabolism 2014

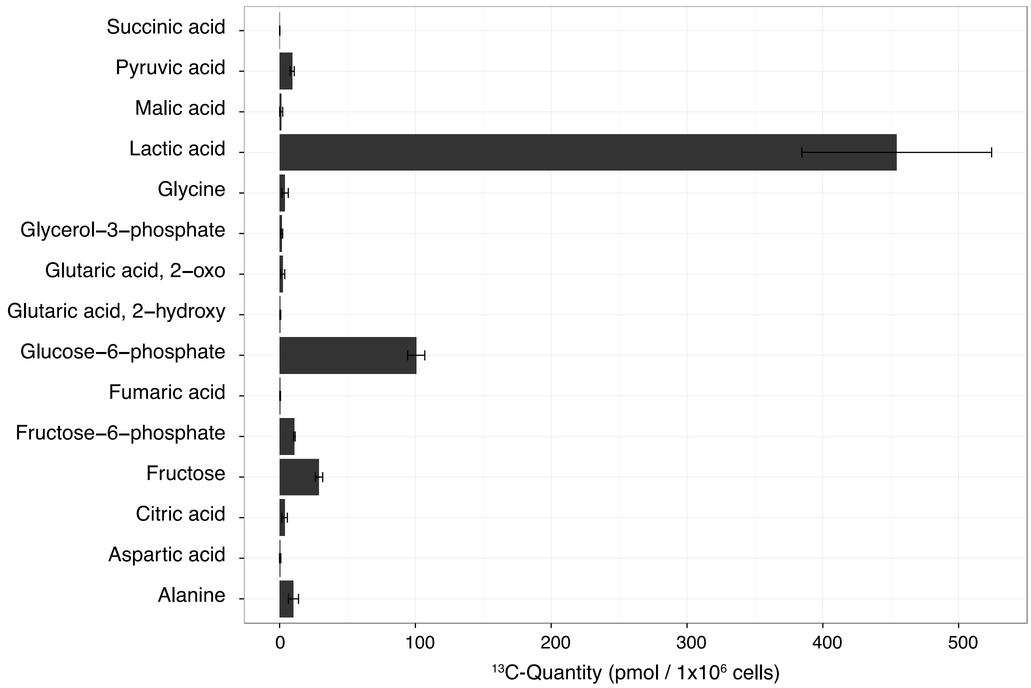

Figure S 5 - Absolute ^{13}C-quantities of intracellular metabolites in T98G cells.
Data derived from the reproducibility experiment (see Methods section and supplement table 6).

Additional file 1
Decoding the dynamics of cellular metabolism and the action of 3-bromopyruvate and 2-deoxyglucose using pulsed stable isotope-resolved metabolomics
Pietzke and Zasada et al., Cancer and Metabolism 2014

Table S 11 – Comparison of carbon routing within the CCM of different cell lines.
The labeled quantities of metabolites after ^{13}C-Glucose incubation into T98G, HEK293, HeLa and HCT-116 cells reveal differences in carbon routing in the central carbon metabolism. Averages and standard deviations for labeled quantities are shown relative to T98G cells.

	^{13}C-Glucose labeled quantity Average ± STDEV											
Compound	**T98G**			**HEK293**			**HeLa**			**HCT-116**		
3PGA	1.00	±	0.04	2.77	±	0.08	1.98	±	0.01	2.47	±	0.01
Ala	1.00	±	0.22	9.59	±	2.65	2.53	±	0.65	1.62	±	0.63
Cit	1.00	±	0.20	13.32	±	0.32	9.82	±	0.34	17.66	±	0.35
DHAP	1.00	±	0.08	2.51	±	0.26	1.68	±	0.30	3.04	±	0.10
F1P	1.00	±	0.15	0.84	±	0.06	0.95	±	0.21	65.64	±	0.07
F6P	1.00	±	0.06	1.11	±	0.02	0.73	±	0.05	10.89	±	0.05
Fru	1.00	±	0.04	0.32	±	0.01	9.56	±	0.04	12.40	±	0.58
G6P	1.00	±	0.07	3.75	±	0.02	2.34	±	0.04	6.82	±	0.06
Glyc	1.00	±	0.03	0.67	±	0.12	3.96	±	0.09	4.40	±	0.58
Glyc3P	1.00	±	0.09	15.57	±	0.86	1.85	±	0.40	3.78	±	0.00
Lac	1.00	±	0.04	8.88	±	2.56	6.64	±	0.02	12.78	±	0.53
Pyr	1.00	±	0.02	8.34	±	1.10	4.18	±	0.80	10.65	±	0.24
R5P	1.00	±	0.12	1.21	±	0.13	1.21	±	0.07	1.52	±	0.01
Ser	1.00	±	0.21	17.29	±	1.68	5.03	±	0.61	7.06	±	0.93

Additional file 1
Decoding the dynamics of cellular metabolism and the action of 3-bromopyruvate and 2-deoxyglucose using pulsed stable isotope-resolved metabolomics
Pietzke and Zasada et al., Cancer and Metabolism 2014

Table S 12 – 3-Bromopyruvate treatment rearranges central carbon metabolism in T98G cells.
T98G cells were treated for 12 min with 2 mM 3-Bromopyruvate and labeled for 3 minutes with u-^{13}C-glucose. Fold changes of peak intensity and ^{13}C-label incorporation are shown relative to control. Two-sided, heteroscedastic t-test indicates significant changes (+++ < 0.005, ++ < 0.01, + < 0.05, n.s. = not significant, *n.d.* = not detected).

	Fold changes relative to control						**% Change relative to control**						**T-Test**					
Compound	**Peak intensity**		**Label incorporation**		**Label inc. x intensity**		**Peak intensity**		**Label incorporation**		**Label inc. x intensity**		**Peak intensity**		**Label incorporation**		**Label inc. x intensity**	
	15min	**30 min**	**15min**	**30 min**	**15min**	**30 min**	**15min**	**30 min**	**15min**	**30 min**	**15min**	**30 min**	**15min**	**30 min**	**15min**	**30 min**	**15min**	**30 min**
G6P	0,8	1,7	0,34	0,25	0,28	0,43	-17	68	-66	-75	-72	-57	n.s.	+++	+++	+++	+++	+++
F6P	3,2	8,2	0,10	0,07	0,31	0,55	224	722	-90	-93	-69	-45	+++	+++	+++	+++	+++	+++
F1,6-BP	3,9	3,4	0,37	0,44	1,07	1,68	285	240	-63	-56	6,8	68,0	++	+	++	+++	n.s.	+
F1P	0,7	1,2	1,13	0,70	0,57	0,59	-26	21	13	-30	-43	-41	+	n.s.	n.s.	+	n.s.	n.s.
Fru	1,0	1,1	0,30	0,30	0,30	0,34	1	11	-70	-70	-70	-66	n.s.	n.s.	+++	+++	+++	+++
6PG	4,5	5,1	*n.d.*	*n.d.*	*n.d.*	*n.d.*	355	413	*n.d.*	*n.d.*	*n.d.*	*n.d.*	+++	+++				
3PGA	*n.d.*	0,3	*n.d.*	0,07	*n.d.*	0,03	*n.d.*	-69	*n.d.*	-93	*n.d.*	-96,5		+++				
Pyr	1,0	1,0	0,10	0,05	0,05	0,04	-2	-1	-90	-95	-94,8	-95,8	n.s.	n.s.	+++	+++	+++	+++
Lac	1,1	0,9	0,036	0,028	0,039	0,025	6	-9	-96,4	-97,2	-96,1	-97,5	n.s.	n.s.	+++	+++	+++	+++
Glyc3P	0,8	0,7	*n.d.*	*n.d.*	*n.d.*	n.d	-16	-28	*n.d.*	*n.d.*	*n.d.*	*n.d.*	n.s.	+++				
Glyc	1,1	1,1	*n.d.*	*n.d.*	*n.d.*	n.d	12	7	*n.d.*	n.d	*n.d.*	n.d	+++	+				
Ala	3,6	4,2	0,05	0,07	0,19	0,23	257	324	-95	-93	-81	-77	+++	+++	+++	+++	+++	+++
Ser	0,8	1,1	*n.d.*	*n.d.*	*n.d.*	*n.d.*	-20	8	*n.d.*	*n.d.*	*n.d.*	*n.d.*	n.s.	n.s.				
Cit	0,5	0,8	0,094	0,11	0,06	0,12	-49	-24	-90,6	-89	-94,1	-87,6	+++	n.s.	+++	+++	+++	+++
aKG	1,4	1,6	*n.d.*	*n.d.*	*n.d.*	n.d	40	58	*n.d.*	n.d	*n.d.*	n.d	+++	+++				
Succ	1,2	1,0	*n.d.*	*n.d.*	*n.d.*	n.d	17	4	*n.d.*	n.d	*n.d.*	n.d	++	n.s.				
Fum	0,4	0,4	*n.d.*	*n.d.*	*n.d.*	n.d	-64	-64	*n.d.*	n.d	*n.d.*	n.d	+++	+++				
Mal	0,3	0,3	*n.d.*	*n.d.*	*n.d.*	n.d	-72	-69	*n.d.*	n.d	*n.d.*	n.d	+++	+++				

Additional file 1
Decoding the dynamics of cellular metabolism and the action of 3-bromopyruvate and 2-deoxyglucose using pulsed stable isotope-resolved metabolomics
Pietzke and Zasada et al., Cancer and Metabolism 2014

Table S 13 – Effect of 2-Deoxyglucose on the central carbon metabolism of T98G cells.
T98G cells were incubated with two different concentrations of 2-Deoxyglucose for 15 min. Rearrangement of metabolism were monitored by ^{13}C-glucose incorporation for 3 minutes. Fold changes of peak intensity and ^{13}C-label incorporation are shown relative to control. Two-sided, heteroscedastic t-test indicates significant changes (+++ < 0.005, ++ < 0.01, + < 0.05, n.s. = not significant, *n.d.* = not detected).

	Fold changes relative to control						**% Change relative to control**						**T-Test**					
Compound	**Peak intensity**		**Label Inc.**		**Label Inc. x intensity**		**Peak intensity**		**Label Inc.**		**Label Inc. x intensity**		**Peak intensity**		**Label Inc.**		**Label Inc. x intensity**	
	2mM	**10mM**	**2mM**	**10mM**	**2mM**	**10mM**	**2mM**	**10mM**	**2mM**	**10mM**	**2mM**	**10mM**	**2mM**	**10mM**	**2mM**	**10mM**	**2mM**	**10mM**
G6P	0.8	0.5	1.0	0.9	0.7	0.5	-24	-49	-4.9	-6.3	-28	-53	n.s.	++	n.s.	n.s.	+	+++
F6P	0.7	0.5	1.1	1.0	0.8	0.6	-27	-46	7.8	5.0	-20	-40	n.s.	n.s.	n.s.	n.s.	n.s.	n.s.
Fru	1.1	1.0	0.9	0.8	1.0	0.8	7.9	-0.2	-10.6	-21.7	-3.3	-22.5	n.s.	n.s.	n.s.	n.s.	n.s.	++
3PGA	0.8	*n.d.*	1.1	*n.d.*	0.9	*n.d.*	-16.9	*n.d.*	6.6	*n.d.*	-11.2	*n.d.*	n.s.		n.s.		n.s.	
Pyr	0.7	0.3	1.3	0.8	0.9	0.2	-28.7	-71.1	31.3	-21.8	-6.8	-79.0	+	+++	+++	n.s.	n.s.	+++
Lac	0.8	0.7	1.2	0.8	1.0	0.6	-19.6	-28.5	20.2	-17.5	-4.7	-41.0	n.s.	+++	n.s.	+	n.s.	+++
Glyc3P	0.9	1.1	1.8	1.3	1.7	1.6	-8.1	14.3	78.2	26.6	72.9	57.2	n.s.	n.s.	+	n.s.	n.s.	n.s.
Glyc	1.0	1.1	*n.d.*	*n.d.*	*n.d.*	*n.d.*	-3.8	5.3	*n.d.*	*n.d.*	*n.d.*	*n.d.*	n.s.	n.s.				
Ala	1.1	0.8	1.7	1.1	1.3	0.6	11.0	-15.8	70.2	5.3	31.9	-44.6	n.s.	n.s.	n.s.	n.s.	n.s.	n.s.
Ser	0.8	0.7	*n.d.*	*n.d.*	*n.d.*	*n.d.*	-17.7	-31.8	*n.d.*	*n.d.*	*n.d.*	*n.d.*	n.s.	+	n.s.	n.s.		
Cit	1.3	1.9	1.7	1.4	2.2	2.5	30.0	85.6	66.7	36.8	115.4	152.6	n.s.	+++	+++	n.s.	+++	+++
aKG	1.0	0.5	*n.d.*	*n.d.*	*n.d.*	n.d	-0.1	-47.5	*n.d.*	n.d	*n.d.*	n.d	n.s.	++				
Succ	0.8	0.8	*n.d.*	*n.d.*	*n.d.*	n.d	-17.3	-15.3	*n.d.*	n.d	*n.d.*	n.d	+	+				
Fum	0.9	0.6	1.1	1.0	1.0	0.6	-6.2	-38.9	13.1	-2.9	3.1	-41.5	n.s.	+++	n.s.	n.s.	n.s.	n.s.
Mal	0.9	0.6	1.4	1.1	1.2	0.6	-7.2	-40.6	37.2	11.3	23.1	-35.8	n.s.	+++	n.s.	n.s.	n.s.	n.s.

Additional file 1
Decoding the dynamics of cellular metabolism and the action of 3-bromopyruvate and 2-deoxyglucose using pulsed stable isotope-resolved metabolomics
Pietzke and Zasada et al., Cancer and Metabolism 2014

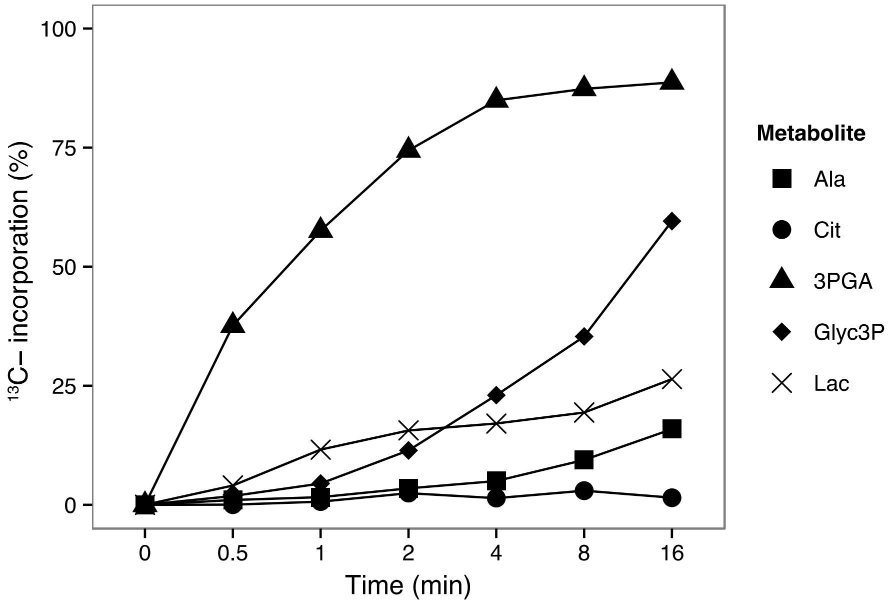

Figure S 6 - Time dependency of ^{13}C-label incorporation into intermediates of the central carbon metabolism.
HEK293 cells, grown in DMEM supplemented with 10 % FBS, 2.5 g/L glucose, and 4 mM glutamine, were incubated with ^{13}C-glucose up to 16 min. Harvest, metabolite extraction, GC-MS measurement and determination of ^{13}C-label incorporation were done as described in the Methods section.

Additional file 1
Decoding the dynamics of cellular metabolism and the action of 3-bromopyruvate and 2-deoxyglucose using pulsed stable isotope-resolved metabolomics
Pietzke and Zasada et al., Cancer and Metabolism 2014

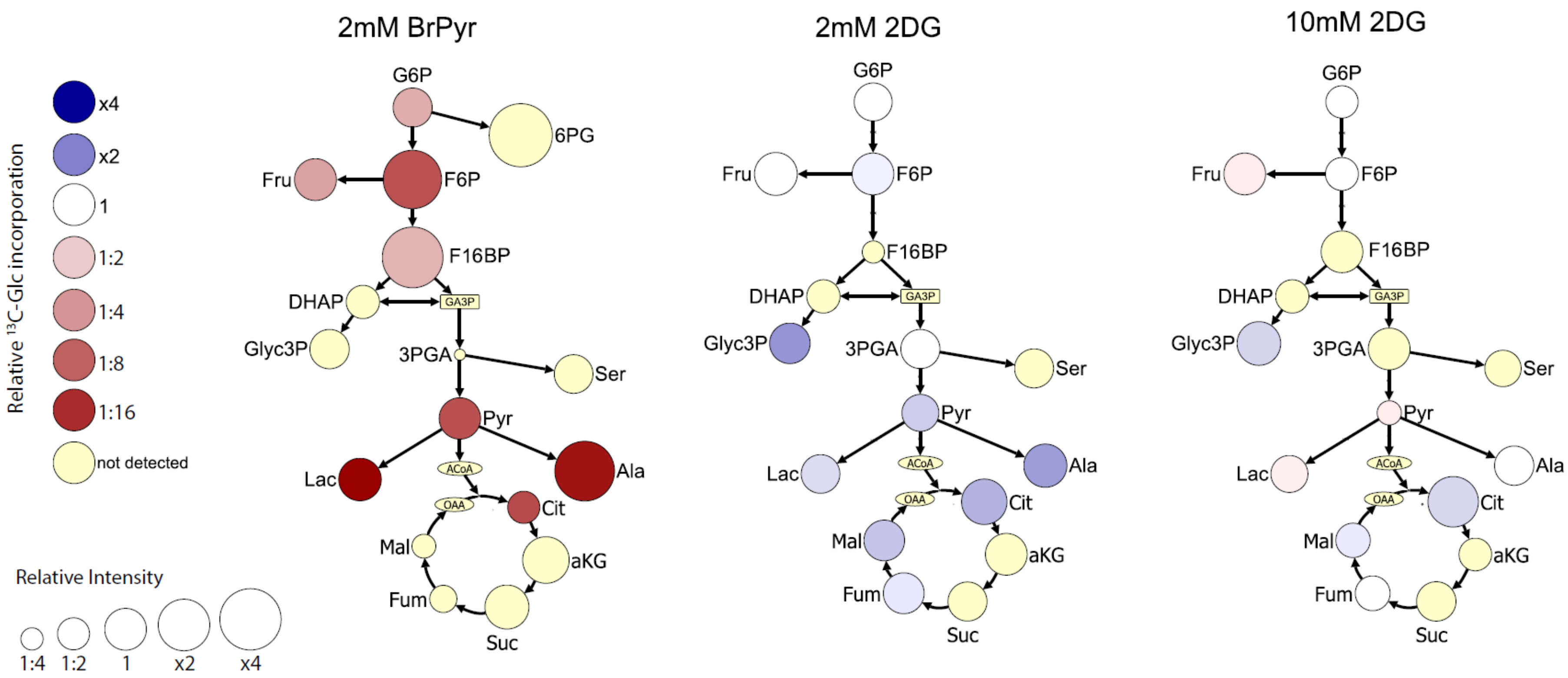

Figure S 7 – Graphical representation of small molecule inhibitor induced rearrangement of central carbon metabolism.
The incorporation of ^{13}C-glucose and abundance of metabolites are presented by color or size relative to the untreated control after 15 minutes of inhibitor treatment and 3 min of ^{13}C-glucose incubation.

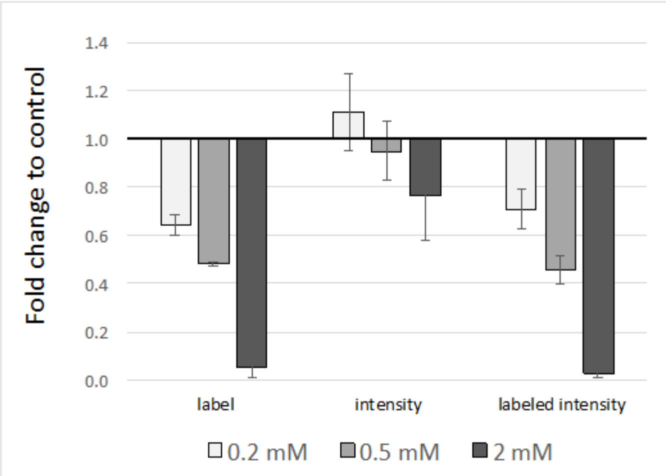

Figure S 8 - Concentration dependency of BrPyr induced inhibition in carbon flow from ^{13}C-glucose to lactate.

Three different concentrations of 3-Bromopyruvate were applied for 15 minutes to T98G cells and incorporation of u-^{13}C-glucose was monitored for 3 minutes in 3 biological replicates. Fold change of incorporated label, intensity (peak area) and labeled intensity were plotted relative to an untreated control.

Additional file 1
Decoding the dynamics of cellular metabolism and the action of 3-bromopyruvate and 2-deoxyglucose using pulsed stable isotope-resolved metabolomics
Pietzke and Zasada et al., Cancer and Metabolism 2014

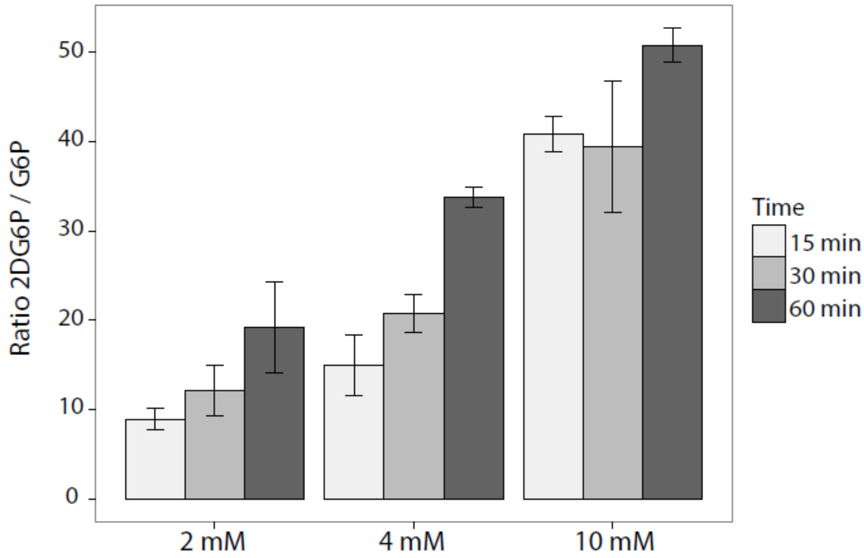

Figure S 9 **-** Time and concentration dependent accumulation of 2-deoxyglucose-6-phosphate (2DG-P). Shown are averages of ratios of two biological replicates measured in two technical replicates.